

## Prediction of ordering and spontaneous rotation of epitaxial habits in substrate-coherent InGa<sub>N</sub> and GaAsSb

Jefferson Zhe Liu, Giancarlo Trimarchi, and Alex Zunger

Citation: *Applied Physics Letters* **95**, 081901 (2009); doi: 10.1063/1.3200234

View online: <http://dx.doi.org/10.1063/1.3200234>

View Table of Contents: <http://scitation.aip.org/content/aip/journal/apl/95/8?ver=pdfcov>

Published by the AIP Publishing

### Articles you may be interested in

X-ray photoelectron spectroscopy analysis of TlInGaAsN semiconductor system and their annealing-induced structural changes

J. Appl. Phys. **108**, 123524 (2010); 10.1063/1.3525979

Strain-induced nitrogen incorporation in atomic layer epitaxy growth of InAsN/GaAs quantum wells using metal organic chemical vapor deposition

Appl. Phys. Lett. **95**, 051102 (2009); 10.1063/1.3193663

Midinfrared photoreflectance study of InAs-rich InAsSb and GaInAsPSb indicating negligible bowing for the spin orbit splitting energy

Appl. Phys. Lett. **90**, 172106 (2007); 10.1063/1.2728752


Metalorganic molecular beam epitaxy of (In)GaAsN with dimethylhydrazine

J. Appl. Phys. **91**, 56 (2002); 10.1063/1.1419206


High rate epitaxial lift-off of InGaP films from GaAs substrates

Appl. Phys. Lett. **76**, 2131 (2000); 10.1063/1.126276


Frustrated by old technology?



Is your AFM dead and can't be repaired?



Sick of bad customer support?



**It is time to upgrade your AFM**

Minimum \$20,000 trade-in discount for purchases before August 31st

**Asylum Research is today's technology leader in AFM**

**OXFORD INSTRUMENTS**

*The Business of Science®*

dropmyoldAFM@oxinst.com

# Prediction of ordering and spontaneous rotation of epitaxial habits in substrate-coherent InGaN and GaAsSb

Jefferson Zhe Liu, Giancarlo Trimarchi, and Alex Zunger<sup>a)</sup>

National Renewable Energy Laboratory, Golden, Colorado 80401, USA

(Received 2 June 2009; accepted 17 July 2009; published online 24 August 2009)

Coherently strained  $\text{In}_{0.5}\text{Ga}_{0.5}\text{N}$  on GaN and CaO substrates are theoretically predicted to show stable ordering in the chalcopyrite structure, as is  $\text{Ga}_2\text{AsSb}$  on GaAs and InP substrates. Depending on the substrate and the film concentration, we predict a spontaneous rotation of the stablest chalcopyrite film axis from perpendicular to parallel to the (001) substrate. © 2009 American Institute of Physics. [DOI: 10.1063/1.3200234]

Epitaxial evaporation of multiple elements onto a fixed substrate<sup>1</sup> has become the method of choice for making high quality crystalline semiconductor films in devices. It is now apparent that such coherent epitaxial growth not only produces greater purity and provides better process control relative to liquid phase or melt growth, but that in fact it corresponds to a different thermodynamic state of the system. There are three major factors distinguishing epitaxial gas-phase growth from non-epitaxial (substrate free) melt growth, the former showing (i) lattice-coherence constraint from the substrate, (ii) exposed surfaces (e.g., possibly leading to reconstruction), and (iii) substrate-film interfaces (leading to atomic interdiffusion and exchange).<sup>2</sup> In light emitting diodes, diode lasers, and III-V multijunction solar cell applications,<sup>3–5</sup> the films are typically 1  $\mu\text{m}$  or more thick and thus the nonideality factors at the substrate-film interfaces [(iii) above] and at the exposed surface [(ii) above] can be assumed negligible. As long as there is coherence with the substrate, the epitaxial constraint from the substrate becomes dominant in deciding the thermodynamic state of such alloy films.<sup>2,6–10</sup>

Figure 1 illustrates the way that a substrate can alter the thermodynamic state of an alloy film made of cubic (In,Ga)N. The blue and red lines show the first-principles calculated (see details below) total energies of an ordered compound  $\text{InGa}_2\text{N}_2$  in the chalcopyrite (CH) structure versus the lattice constant  $a_s$  of the substrate on which it is epitaxially grown. The ordered CH, coherent with the substrate, has two epitaxial habits: one perpendicular  $\perp$  and one parallel  $\parallel$  to the substrate [Figs. 1(b) and 1(c)]. As  $a_s$  deviates from the equilibrium lattice constants  $\bar{a}_{\parallel}$  and  $\bar{a}_{\perp}$  of each epitaxial habit, the energies  $E_{\text{CH}\parallel}$  and  $E_{\text{CH}\perp}$  of  $\parallel$  and  $\perp$  CH, respectively, rise. The black line in Fig. 1 marks  $E_{\text{InN+GaN}}^{\text{epi}}$  which is the energy of equivalent amounts of the strained binary constituents versus  $a_s$

$$E_{\text{InN+GaN}}^{\text{epi}}(a_s) = \frac{1}{2}[E_{\text{InN}}^{\text{epi}}(a_s, \hat{G}) + E_{\text{GaN}}^{\text{epi}}(a_s, \hat{G})], \quad (1)$$

where  $E_{\text{GaN}}^{\text{epi}}(a_s, \hat{G})$  is the energy of GaN confined to the lattice constant  $a_s$  in the substrate  $\hat{G}$  plane and the remaining lattice (and cell-internal) degrees of freedom are relaxed. We see from Fig. 1 that epitaxy can increase the energy  $E_{\text{InN+GaN}}^{\text{epi}}$  of the constituents more than the energy  $E_{\text{CH}}^{\text{epi}}$  of the interme-

diate  $\text{InGa}_2\text{N}_2$  compounds and, consequently, the epitaxial formation energy of CH

$$\delta E_{\text{CH}}^{\text{epi}}(a_s) = E_{\text{CH}}^{\text{epi}}(a_s) - E_{\text{InN+GaN}}^{\text{epi}}(a_s), \quad (2)$$

could become negative (Fig. 1) even if the bulk formation energy of CH

$$\Delta E_{\text{CH}}^{\text{bk}} = E_{\text{CH}}^{\text{bk}} - E_{\text{InN+GaN}}^{\text{bk}} \quad (3)$$

is positive. In Eq. (3),  $E_{\text{InN+GaN}}^{\text{bk}}$  is the average of the energies of the constituents each at its own, free-floating bulk lattice constant. This “epitaxial-stabilization” effect leads to a variety of fascinating phenomena, such as the appearance of ordered epitaxial phases without a counterpart in the bulk phase diagram,<sup>2,11</sup> as well as to the enhancement in solubility under epitaxial condition,<sup>9</sup> or the change in the equilibrium alloy composition (“lattice latching”) relative to bulk growth.<sup>6</sup> Such effect exists when the film thickness is below a critical thickness.<sup>2</sup>

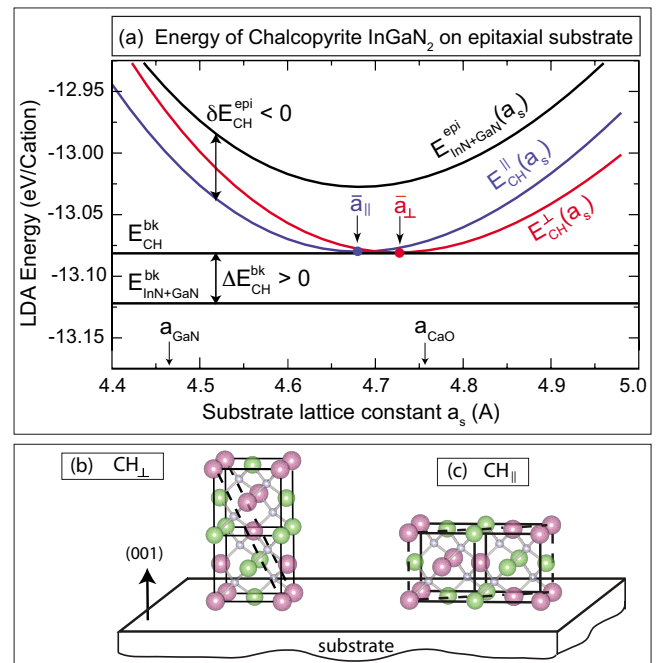


FIG. 1. (Color online) (a) Total energy of two epitaxial habits of CH  $\text{InGa}_2\text{N}_2$  as a function of the substrate lattice constant  $a_s$ . The energy of bulk CH  $E_{\text{CH}}^{\text{bk}}$  and the energy of the bulk  $\text{InN+GaN}$  constituents  $E_{\text{InN+GaN}}^{\text{bk}}$  are shown as references. [(b) and (c)] show the structure of the two habits of CH:  $\parallel$  and  $\perp$ .

<sup>a)</sup>Electronic mail: alex.zunger@nrel.gov.

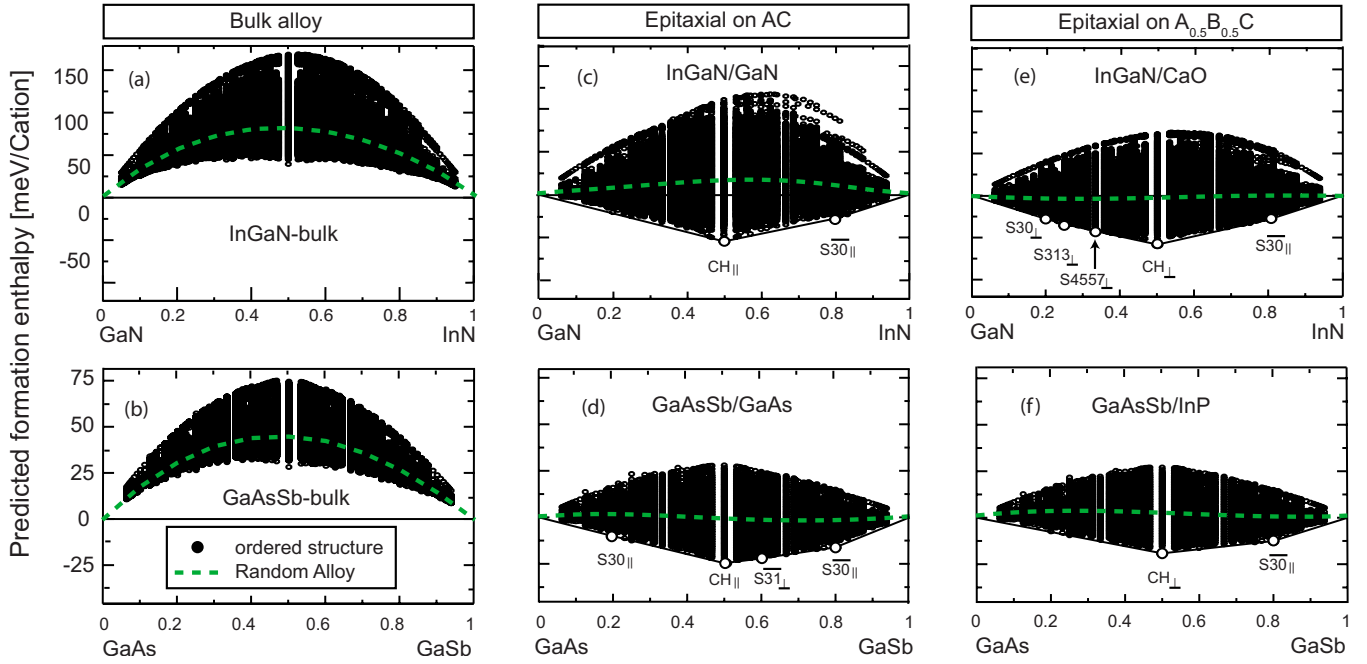


FIG. 2. (Color online) Formation energies of bulk and epitaxial (In,Ga)N and Ga(As,Sb) alloys as calculated by cluster expansions. [(a) and (b)] show the bulk formation energy. [(c) and (d)] depict the epitaxial formation energies of (In,Ga)N and Ga(As,Sb) grown on end-point substrate. [(e) and (f)] show the epitaxial formation energy of the two alloys grown on midpoint substrates.

Attempts to develop a theoretical approach describing epitaxial thermodynamic phenomenology are rare.<sup>6–10</sup> Most<sup>6–8</sup> only considered the random alloy phase, ignoring the fact that  $\delta E^{\text{epi}} < 0$  could lead to a variety of long-range ordered phases. A few approaches<sup>9,10</sup> consider the possibility of epitaxial ordered phases, but ignore<sup>9</sup> or average-over<sup>10</sup> the habits that have different orientations (e.g.,  $\parallel$  or  $\perp$ ) to the substrate. We have recently developed an epitaxial cluster-expansion (CE) method that describes the energy of both random alloys and the ensuing ordered epiphases as well as their habits.<sup>12</sup> Here, we apply this technique to prototypical *mixed cation* (In,Ga)N and *mixed-anion* Ga(As,Sb) alloys comparing bulk and epitaxial cases side by side on a range of substrates. In addition to showing the ordering induced by epitaxy in the structures of (In,Ga)N on GaN and CaO and of Ga(As,Sb) on GaAs and InP, we focus on the orientation of the coherent film (“habit”) versus substrate. We predict a spontaneous switch between the parallel-to-substrate ( $\parallel$ ) and perpendicular-to-substrate ( $\perp$ ) film habits as a function of (i) the substrate lattice constant at fixed film composition and (ii) as the film composition changes on a fixed substrate. We explain this remarkable spontaneous rotation by the tetragonal ratio of the bulk structure. The computational method employed here is described in Ref. 12. It is based on a “cluster expansion”<sup>13</sup> whereby the energy of a given configuration  $\sigma$  (e.g., assignment of Ga and In atoms onto lattice sites) is parametrized as a sum of pairwise plus many-body interactions whose magnitude and range are determined by fitting the cluster-expansion energies  $\{E_{\text{CE}}(\sigma)\}$  of a set  $\{\sigma_0\}$  of about 50 structures to  $\{E_{\text{LDA}}(\sigma)\}$  energies calculated by the local density approximation<sup>14</sup> (LDA) using ultrasoft pseudopotentials as implemented in the VASP (Ref. 15) code. For epitaxially coherent films, the structures  $\sigma$  are substrate coherent with a particular epitaxial habit. For example, CH is a superlattice (SL) structure composed of alternate atomic bilayers along the three (201)-equivalent crystallographic directions;

(201), (210), and (102). Figures 1(b) and 1(c) show, respectively, the (201) (i.e.,  $\perp$ ) and the (210) (i.e.,  $\parallel$ ) habits of CH on a (001) substrate [where the (102) habit is degenerate with the (210) one]. While in bulk form these habits have the same energy, their epitaxial strain energies are generally different [Fig. 1(a)], rendering these bulk-equivalent configurations epitaxially distinct. Once we obtain  $E_{\text{CE}}(\sigma)$  for any configuration  $\sigma$ , an exhaustive enumeration method is then employed to search the ground-state structures. The LDA energies of the newly predicted ground-state structures are then input into the next CE iterations until the predictions of our CE agree with the direct LDA calculations.

**Epitaxial ground-state structures:** Fig. 2 shows the CE-calculated formation energies of  $\sim 2^{16}$  structures of (In,Ga)N and Ga(As,Sb) alloys both under bulk [Figs. 2(a) and 2(b)] and epitaxial [Figs. 2(c)–2(f)] conditions. For each epitaxial alloy, we use two substrates: an “end-point” substrate [Figs. 2(c) and 2(d)], i.e., one of the pure constituents as substrate, and a “midpoint” substrate [Figs. 2(e) and 2(f)], i.e., a substrate whose lattice constant is close to the natural film lattice constant of  $x \sim 0.50$ . The black lines encompassing all structures in Figs. 2(c)–2(e) are the energy convex hulls whose breaking points are the ground-state structures of the corresponding alloy. The main observations are as follows:

(i) *Confirming previously known or suspected trends:* The phase separation behavior in bulk ( $\Delta E_{\text{bulk}} > 0$ ) is transformed under epitaxial conditions to an ordering behavior ( $\delta E_{\text{epi}} < 0$ ) with several ground-state structures that appear across the whole composition interval. All the identified ground-state structures (Fig. 2) are (201) SLs. At  $x=0.50$  we find a universal epitaxial ground-state structure—CH [Figs. 1(b) and 1(c)] as previously found.<sup>2,10,19</sup> For many III-V zinc-blende bulk alloys, CH was identified to be the structure at  $x=0.50$  best able to accommodate strain resulting from the mismatch between the AC and BC bond lengths.<sup>16</sup> At  $x=0.80$ , we found the second universal epitaxial ground-state

structure S30:  $(AC)_1/(BC)_4$  (201) SL structure.

(ii) *Spontaneous rotation of epitaxial habits*: Fig. 2 shows that when one uses an end-point substrate (e.g., InGa<sub>N</sub>-on-GaN or GaAsSb-on-GaAs), provided there is coherence, the lowest energy CH habit is the  $\parallel$  one [i.e., (210)]. However, when the substrate changes to a midpoint one (as in InGa<sub>N</sub>-on-CaO or GaAsSb-on-InP), the lowest energy film habit becomes the  $\perp$  one [i.e., (201)]. A similar rotation of the most stable film habit occurs also when the film composition changes while keeping fixed the substrate, e.g., in the InGa<sub>N</sub>-on-CaO system, the ordered S30  $(AC)_4/(BC)_1$  at  $x=0.20$  is the lowest energy for habit  $\perp$  whereas counterpart S30 at  $x=0.80$  is the lowest energy for habit  $\parallel$ .

*Explanation of the habit rotation*: Inspection of the energy versus  $a_s$  curves of epitaxial CH $_{\parallel}$  and CH $_{\perp}$  in Fig. 1(a) shows almost identical curvatures (i.e., similar elastic moduli for the two habits) but different minima (i.e., equilibrium values of  $\bar{a}_{\parallel}$  and  $\bar{a}_{\perp}$ ). This indicates that the different lattice mismatches  $a_s - \bar{a}_{\parallel}$  and  $a_s - \bar{a}_{\perp}$  of epitaxial CH $_{\parallel}$  and CH $_{\perp}$ , respectively, on the same substrate induce the energy difference. Here we will demonstrate that the tetragonal ratio  $\eta = c/2a$  of bulk CH leads to such a difference in  $\bar{a}_{\parallel}$  versus  $\bar{a}_{\perp}$ . Bulk CH usually has<sup>17</sup>  $\eta = c/2a \neq 1$ . The habit CH $_{\parallel}$  [Fig. 1(c)] thus has two different lattice constants  $a$  and  $c/2$  [along the (010) and (100) directions, respectively] in the (001) plane. When CH $_{\parallel}$  is grown on the (001) plane of a cubic substrate, the ensuing epitaxial strain energy  $E^{SS}(a_s)$  can be expanded as a polynomial of strain<sup>18</sup>

$$E_{\parallel}^{SS}(a_s) = S(C)\lambda^2 + \frac{1}{2}[Bq_{001} + S(C)\lambda^2]\left(\frac{a_s - \bar{a}_{\parallel}}{\bar{a}_{\parallel}}\right)^2 + \dots \quad (4)$$

The corresponding equilibrium lattice constant is

$$\bar{a}_{\parallel} = a[1 + s(C)\lambda] = \frac{c}{2}\{1 - [1 - s(C)]\lambda\}, \quad (5)$$

where  $\lambda = 1 - \eta$ ,  $B$  is the bulk modulus, and  $q_{001}$  is the epitaxial strain reduction factor<sup>2</sup> along the (001) direction for CH $_{\parallel}$ . Here,  $S(C)\lambda^2$  is the energy to deform the two different lattice constants of CH $_{\parallel}$  in the (001) plane to make them equal to  $\bar{a}_{\parallel}$  and  $C$  is the elastic constant tensor of CH $_{\parallel}$ . The parameter  $s(C)$  is comprised between 0 and 1, thus the equilibrium  $\bar{a}_{\parallel}$  is intermediate between  $a$  and  $c/2$ .

An expression similar to Eq. (4) holds for the epitaxial strain energy of CH $_{\perp}$  but the  $\lambda^2$  terms drop as the lattice constants of CH $_{\perp}$  along the in-plane directions are equal, i.e.,  $\lambda=0$  [Fig. 1(b)], and the equilibrium lattice constant  $\bar{a}_{\perp}$  is the same as that of equilibrium bulk CH one, i.e.,  $\bar{a}_{\perp} = a$ . From Eqs. (4) and (5), we see that the term that is function of  $\eta = \lambda + 1$  is a second order correction to the elastic modulus but a first order contribution to the equilibrium lattice constant  $\bar{a}$ . Therefore, in Fig. 1(a) the curvature of  $E^{SS}(a_s)$  is almost identical for the  $\parallel$  and  $\perp$  habits, whereas the difference between  $\bar{a}_{\parallel}$  and  $\bar{a}_{\perp}$  is significant. As a result the energy order of different habits is determined by the different lattice mismatches with respect to a given substrate. Bulk CH has  $\lambda \sim -1.5\%$  for (In,Ga)N and Ga(As,Sb) In Fig. 1(a),  $a_{\text{GaN}} < \bar{a}_{\parallel}(\text{CH}) < \bar{a}_{\perp}(\text{CH})$ , thus CH $_{\parallel}$  has lower strain energy on GaN substrate than CH $_{\perp}$ . On the CaO substrate,  $\bar{a}_{\parallel}(\text{CH}) < \bar{a}_{\perp}(\text{CH}) < a_{\text{CaO}}$  yields lower energy of CH $_{\perp}$  than CH $_{\parallel}$ . We

found a similar situation for Ga(As,Sb) epitaxial alloys. Changing the substrate, therefore, alters the energy order of the habits of CH. For InGa<sub>N</sub>-on-CaO, both the S30 and S30 structures have  $\eta < 1$  and thus  $\bar{a}_{\parallel} < \bar{a}_{\perp}$ . Moreover, we have  $\bar{a}_{\parallel}(\text{S30}) < \bar{a}_{\perp}(\text{S30}) < a_{\text{CaO}}$  and  $a_{\text{CaO}} < \bar{a}_{\parallel}(\text{S30}) < \bar{a}_{\perp}(\text{S30})$ . Therefore S30 $_{\perp}$  and S30 $_{\parallel}$  have each lower energy than the respective opposite habits. Structure S31 in the GaAsSb-on-GaAs system is the only exception in all of the ground-state structures that has  $\eta > 1$  in its bulk structure hence  $\bar{a}_{\perp} < \bar{a}_{\parallel}$ . Thus, in Figs. 2(c) and 2(d), all the ground-state structures have habits  $\parallel$  except structure S31.

In summary, we predicted (1) a number of long range ordered ground-state structures in epitaxial (In,Ga)N coherent on GaN and CaO and Ga(As,Sb) coherent on GaAs and InP; (2) a spontaneous switch between the parallel-to-substrate ( $\parallel$ ) and perpendicular-to-substrate ( $\perp$ ) epitaxial habits of a ground-state structure as a function of the different substrate, i.e., end-point and midpoint substrates, and as a function of the film composition on a fixed substrate. Such a switch can be explained by the tetragonal ratio  $\eta \neq 1$  of the corresponding bulk structure. Our results show that the epitaxial strain alters the thermodynamics of an alloy with respect to bulk conditions, transforming it from phase separation to an ordering one.

We thank A. Ptak for many helpful discussions on epitaxy of (In,Ga)N. This research was funded by the U.S. Department of Energy, Office of Science, DMSE, under Contract No. DE-AC36-99GO10337 and the LDRD program of NREL.

<sup>1</sup>J. Y. Tsao, *Materials Fundamentals of Molecular Beam Epitaxy* (Academic, New York, 1993).

<sup>2</sup>A. Zunger and S. Mahajan, in *Handbook on Semiconductors*, edited by T. S. Moss (North-Holland, Amsterdam, 1992), Vol. 3, p. 1399.

<sup>3</sup>See, i.e., <http://www.philipslumileds.com/products/luxeon/luxeonrebel>.

<sup>4</sup>S. Nakamura, M. Senoh, S. Nagahama, N. Iwasa, T. Yamada, T. Matsushita, H. Kiyoku, Y. Sugimoto, T. Kozaki, H. Umemoto, M. Sano, and K. Chocho, *Appl. Phys. Lett.* **72**, 211 (1998).

<sup>5</sup>G. F. Geisz, S. Kurtz, M. W. Wanlass, J. S. Ward, A. Duda, D. J. Friedman, J. M. Olson, W. E. McMahon, T. E. Moriarty, and J. T. Kiehl, *Appl. Phys. Lett.* **91**, 023502 (2007).

<sup>6</sup>G. B. Stringfellow, *J. Appl. Phys.* **43**, 3455 (1972).

<sup>7</sup>B. de Cremoux, *J. Phys. (Paris), Colloq.* **43**, C5 (1982); F. Glas, *J. Appl. Phys.* **62**, 3201 (1987).

<sup>8</sup>S. Yu. Karpov, *MRS Internet J. Nitride Semicond. Res.* **3**, 16 (1998).

<sup>9</sup>D. M. Wood and A. Zunger, *Phys. Rev. Lett.* **61**, 1501 (1988); *Phys. Rev. B* **40**, 4062 (1989).

<sup>10</sup>L. K. Teles, L. G. Ferreira, L. M. R. Scolfaro, and J. R. Leite, *Phys. Rev. B* **69**, 245317 (2004).

<sup>11</sup>H. R. Jen, M. J. Churng, and G. B. Stringfellow, *Appl. Phys. Lett.* **48**, 1603 (1986); T. S. Kuan, W. I. Wang, and E. L. Wilkie, *ibid.* **51**, 51 (1987); N. Nakayama and H. Fujita, in *GaAs and Related Compounds 1985*, Institute of Physics Conference Series Vol. 79, edited by M. Fujimoto (Hilger, London, 1986).

<sup>12</sup>J. Z. Liu and A. Zunger, *J. Phys.: Condens. Matter* **21**, 295402 (2009).

<sup>13</sup>D. B. Laks, L. G. Ferreira, S. Froyen, and A. Zunger, *Phys. Rev. B* **46**, 12587 (1992).

<sup>14</sup>J. P. Perdew and A. Zunger, *Phys. Rev. B* **23**, 5048 (1981).

<sup>15</sup>G. Kresse and J. Fürthmüller, *Comput. Mater. Sci.* **6**, 15 (1996).

<sup>16</sup>J. Z. Liu, G. Trimarchi, and A. Zunger, *Phys. Rev. Lett.* **99**, 145501 (2007).

<sup>17</sup>J. E. Jaffe and A. Zunger, *Phys. Rev. B* **28**, 5822 (1983).

<sup>18</sup>S. P. Timoshenko and J. N. Goodier, *Theory of Elasticity* (McGraw-Hill, New York, 1970).

<sup>19</sup>J. Z. Liu and A. Zunger, *Phys. Rev. B* **77**, 205201 (2008).